Eur. Phys. J. D **37**, 59–66 (2006)
DOI: 10.1140/epjd/e2005-00259-5

THE EUROPEAN PHYSICAL JOURNAL D

Collision-induced absorption by D_2 pairs in the first overtone band at 77, 201 and 298 K

M. Abu-Kharma[a], P.G. Gillard, and S.P. Reddy[b]

Department of Physics and Physical Oceanography, Memorial University of Newfoundland, St. John's, Newfoundland, A1B 3X7, Canada

Received 22 June 2005
Published online 27 September 2005 –

Abstract. Collision induced absorption (CIA) spectra of pure D_2 in the first overtone region from 5250 to 7250 cm^{-1}, recorded at 77, 201 and 298 K, have been analyzed. The observed spectra at 77, 201 and 298 K were modelled by a total of 92, 214 and 267 components respectively of double vibrational transitions at room temperature of the type $X_2(J)+X_0(J)$ and $X_1(J)+X_1(J)$, where X is O, Q or S transitions. Profile analyses of the spectra were carried out using the Birnbaum-Cohen line-shape function for the individual components of the band, and characteristic line shape parameters were determined from the analysis. The observed and calculated profiles agree well over the whole overtone band, and the agreement is better than 97% in the three cases studied. Binary and ternary absorption coefficients were determined from the integrated absorption of the band.

PACS. 33.20.Ea Infrared spectra – 33.20.-t Molecular spectra – 33.20.Vq Vibration-rotation analysis

1 Introduction

Symmetric diatomic molecules such as H_2 and D_2 have no permanent electric-dipole moment in their ground electronic states and are therefore forbidden to absorb or emit dipole radiation. However, transient electric dipole moment can be induced in a pair of colliding homonuclear molecules due to intermolecular interaction [1], therefore they will be active in the near infrared region. This leads to the formulation of the theory of collision induced absorption (CIA).

CIA has been used to determine the composition of many stellar bodies and to study the force of interaction between the colliding molecules. The rotational-vibrational bands of the CIA spectra of pure gases and gaseous mixtures such as H_2, N_2, CO_2, H_2–He and H_2–N_2 are of considerable interest in astrophysics, especially for spectral studies of planetary atmospheres [2–6]. For more details of the role of collision-induced absorption in the planetary atmospheres see Trafton 1998.

The CIA spectrum of H_2 in the first overtone band in the pure gas was observed in 1951 by Welsh et al. [7] who identified the spectrum as consisting of single vibrational transitions ($\Delta v = v' - v'' = 2 \leftarrow 0$) and double vibrational transitions ($\Delta v = 1 \leftarrow 0$) in each of the colliding pair of molecules. Soon after, the overtone bands of H_2 have been further investigated under different theoretical and experimental conditions by Welsh and co-workers [3,8–10], Silvaggio et al. [11], McKellar [12], Meyer et al. [13] and Reddy et al. [14]. McKellar and Clouter [15] studied the fundamental band of H_2 and D_2 liquids in the regions 4000 to 5000 cm^{-1} and 2900 to 3600 cm^{-1}, respectively. Gustafsson et al. [16] reported the collision-induced absorption spectra of H_2–H_2 at temperatures of 297.5 and 77.5 K in the frequency range 1900 to 2260 cm^{-1} at gas densities ranging from 51 to 610 amagat. McKellar [17–19] studied the infrared spectra of H_2–Ar, HD–Ar, D_2–Ar, CO_2–H_2, H_2–Kr and D_2–Kr.

CIA of the fundamental band of gaseous deuterium was originally studied by Reddy and Cho [20] and Watanabe and Welsh [21]. Later, the fundamental and the overtone bands of D_2 and the binary mixtures of D_2 were investigated under different experimental conditions by Reddy and co-workers [22–26]. The CIA spectra of D_2 in the pure gas and D_2–Ar and D_2–N_2 binary mixtures in the first overtone band were investigated also by Reddy and Kuo [23] who identified the spectrum of D_2–D_2 as consisting of double transitions, where the major contribution to the intensity of the absorption profiles comes from the following double transitions $Q_1(J)+Q_1(J)$, $Q_1(J)+S_1(J)$ and $Q_2(J)+S_0(J)$. A special feature of the spectra was the absence of the isotropic overlap contribution. Recently, the CIA spectrum of D_2 in D_2–N_2 binary mixtures in the first overtone band was reinvestigated and analyzed by Abu-Kharma et al. [27], the spectrum of D_2–N_2 consists of double transitions $X_2(J)$ of $D_2+X_0(J)$ of N_2 and $X_1(J)$ of $D_2+X_1(J)$ of N_2, where X is O, Q or S transition. Also,

[a] e-mail: mkharma@kelvin.physics.mun.ca
[b] e-mail: spreddy@physics.mun.ca

Table 1. The possible quadrupolar transitions of pure D_2 at 77, 201 and 298 K.

Transition	J of the first molecule	J of the second molecule	Number of components
$O_2(J) + Q_0(J)$	2–5	0–5	24
$Q_2(J) + Q_0(J)$[a]	0–5	0–5	35
$S_2(J) + Q_0(J)$	0–5	0–5	36
$Q_2(J) + S_0(J)$	0–5	0–5	36
$S_2(J) + S_0(J)$	0–4	0–4	25
Number of transitions			**156**
$O_1(2) + O_1(2)$	2	2	1
$O_1(J) + Q_1(J)$	2–5	0–5	24
$O_1(J) + S_1(J)$	2–4	0–4	15
$Q_1(J) + Q_1(J)$	0–5	0–5	20
$Q_1(J) + S_1(J)$	0–5	0–5	36
$S_1(J) + S_1(J)$	0–4	0–4	15
Number of transitions			**111**
Total number of components			**267**

[a] $Q_2(0) + Q_0(0)$ is forbidden transition. [b] The number of components given here is for the room temperature case, this number decreases with decreasing temperature.

Abu-Kharma and Reddy studied the first overtone band of D_2 in binary mixtures of D_2–Y, where Y is Ar, Kr and Xe [28].

In the present paper the CIA spectra of the first overtone band of pure D_2 were investigated at 77, 201 and 298 K, the results obtained were compared with previous studies of both D_2 and H_2 in the 1st overtone region. The spectra of pure D_2 at 298 K consist of a total 267 components of double vibrational transitions of the type $X_2(J) + X_0(J)$ and the type $X_1(J) + X_1(J)$, where X is O, Q or S transition. The possible combinations of these transitions are listed in Table 1. The absorption profiles were analyzed using Birnbaum-Cohen (BC) lineshape function [29] for all the possible transitions arising from the quadrupolar-induction mechanism.

2 Experimental details

A two-meter transmission-type stainless steel absorption cell was used to contain the gases [26]. A General Electric FFJ Quartzline lamp housed in a water-cooled brass jacket was the source of continuous infrared radiation. The spectrometer was a Perkin-Elmer Model 112 single-beam double-pass instrument equipped with a LiF prism, an uncooled PbS detector, and a 260 Hz tuning fork chopper (Model L-40, supplied by American Time Products) driven by a Micro-Controlled Stepper Driver (supplied by Technical Services of Memorial University of Newfoundland). A slit width maintained at 60 μm gave a spectral resolution of 12.5 cm^{-1} at 5868 cm^{-1}, the origin of the first overtone band of D_2. The signal detection and amplification system consisted of SR510 lock-in amplifier (supplied by Stanford Research Systems). The entire optical path outside the absorption cell was contained within an airtight Plexiglas box and flushed with dry nitrogen gas in order to minimize the presence of water vapor and to maintain a constant level of background water vapor absorption. Mercury emission lines and water vapor absorption peaks were used for calibration of the spectral region 5250−7250 cm^{-1}. Experiments were carried out with densities in the range 118−450 amagat of D_2. The wave numbers (cm^{-1}) of the quadrupolar transitions were calculated from the molecular constants of D_2 [30].

The densities ρ of D_2 at temperature 201 and 298 K were obtained from a linear least squares fit to the PVT data tabulated by Michels et al. [31], while ρ at 77 K was obtained from a plot of the difference in pressure of H_2 and D_2 against density at 77, 123, 273 and 358 K, for more information see reference [26].

For a given density ρ of D_2 the absorption coefficient at a given wavenumber $\nu(cm^{-1})$ is expressed as

$$\alpha(\nu) = (1/l)\ln[I_0(\nu)/I(\nu)], \quad (1)$$

where l is the sample path length of the absorption cell, and $I_0(\nu)$ and $I(\nu)$ are the intensities transmitted by the empty cell and the cell containing the gas, respectively. Absorption profiles were obtained by plotting $\ln[I_0(\nu)/I(\nu)]$ versus ν. The areas of the enhancement absorption profiles gave the integrated absorption $\int \alpha(\nu)d\nu$ for the band.

3 Absorption coefficients

The basic theory of collision-induced absorption in gases has been developed by van Kranendonk [32–35], Karl et al., Poll and Hunt, and Lewis [36–38]. The integrated absorption coefficient can be expanded in terms of the densities ρ as

$$\int \alpha(\nu)d\nu = \alpha_1\rho^2 + \alpha_2\rho^3 + \cdots \quad (2)$$

ρ is the density of D_2 in amagat units, α_1 is the binary absorption coefficient resulting from binary collisions (two

molecules), and α_2 is the ternary absorption coefficients resulting from ternary collisions (three molecules). The dimensionless absorption coefficient $\widetilde{\alpha}(\nu)$ is defined as

$$\widetilde{\alpha}(\nu) \equiv (\alpha_\nu)/\nu, \tag{3}$$

and expanded as

$$c\int \widetilde{\alpha}(\nu)d\nu = \widetilde{\alpha}_1\rho^2 n_0^2 + \widetilde{\alpha}_2\rho^3 n_0^3 + \cdots \tag{4}$$

where c is the speed of light, and n_0 is Loschmidt's number (2.68676×10^{19} cm^{-3}). The absorption coefficients $\widetilde{\alpha}_1(\mathrm{cm}^6\,\mathrm{s}^{-1})$, $\widetilde{\alpha}_2(\mathrm{cm}^9\,\mathrm{s}^{-1})$, are related to the absorption coefficients in equation (2) by the following

$$\begin{aligned}\widetilde{\alpha}_1(\nu) &= \left(c/n_0^2\right)\alpha_1(\nu)/\overline{\nu},\\ \widetilde{\alpha}_2(\nu) &= \left(c/n_0^3\right)\alpha_2(\nu)/\overline{\nu},\end{aligned} \tag{5}$$

where $\overline{\nu}$ is weighted mean wavenumber of the band given by

$$\overline{\nu} = \frac{\int \alpha(\nu)d\nu}{\int \alpha(\nu)\nu^{-1}d\nu}. \tag{6}$$

The average value of $\overline{\nu}$ for D_2 first overtone band is 6130 ± 7, 6114 ± 4 and 6104 ± 11 cm^{-1} at 77, 201 and 298 K, respectively.

4 Theoretical binary absorption coefficients

The integrated binary absorption coefficient of a specific Lth order multipole-induced transition is given by (Ref. [39])

$$\begin{aligned}\tilde{\alpha}_{Lm} &= (1/\rho^2)\int \frac{\alpha_m(\nu)}{\nu}d\nu\\ &= (4\pi^3 e^2/3hc)n_0^2 a_0^5 (a_0/\sigma)^{2L+1}\widetilde{J}_L X_{Lm}.\end{aligned} \tag{7}$$

Here the quantity X_{Lm} is given by

$$\begin{aligned}X_{Lm} = P_{J_1}P_{J_2}[&C(J_1\ L\ J_1';00)^2\langle v_1J_1 \mid Q_{L_1} \mid v_1'J_1'\rangle^2\\ &\times C(J_2\ 0\ J_2';00)^2\langle v_2J_2 \mid \alpha_2 \mid v_2'J_2'\rangle^2\\ &+ C(J_2\ L\ J_2';00)^2\langle v_2J_2 \mid Q_{L_2} \mid v_2'J_2'\rangle^2\\ &\times C(J_1\ 0\ J_1';00)^2\langle v_1J_1 \mid \alpha_1 \mid v_1'J_1'\rangle^2] + Y_{Lm},\end{aligned} \tag{8}$$

and

$$\widetilde{J}_L(T^*) = 4\pi(L+1)\int_0^\infty x^{-2(L+2)}g_0(x)x^2dx, \tag{9}$$

where m indicates the quantum number characterizing the transition, ρ is the density of the gas in amagat, e is the electron charge, a_0 is the Bohr radius, h is the Planck constant and σ is the intermolecular separation corresponding to the intermolecular potential $V(\sigma) = 0$ where $V(x)$ is the Lennard-Jones pair potential

$$V(x) = 4\epsilon(x^{-12} - x^{-6}). \tag{10}$$

In this equation $x = R/\sigma$, where R is the intermolecular separation, and ϵ is the depth of the potential well. $\widetilde{J}_L = J_q$ for the special case of $L = 2$ and represents the average dependence of the square of the induced dipole moment on R, where

$$T^* = kT/\epsilon, \tag{11}$$

and g_0 is the low density limit of the pair correlation function which in classical limit is given by

$$g_0(x) = e^{-V^*(x)/T^*}, \tag{12}$$

with

$$V^*(x) = V(x)/\epsilon. \tag{13}$$

The normalized Boltzmann factor is written as

$$P_J = \frac{g_T(2J+1)e^{-E_J/kT}}{\sum_J g_T(2J+1)e^{-E_J/kT}}, \tag{14}$$

where g_T is the nuclear statistical weight, $g_T = 6$ and 3 for even and odd J for D_2. E_J is the rotational energy. The squares of the Clebsch-Gordan coefficients are represented by the following equations:
for the Q($\Delta J = 0$, $L = 0$) transitions:

$$C(J\ 0\ J';00)^2 = \delta_{JJ'} = \begin{cases}1 \text{ if } J = J'\\ 0 \text{ if } J \neq J',\end{cases} \tag{15}$$

for the O($\Delta J = -2, L = 2$) transitions:

$$C(J\ 2\ [J-2];00)^2 = \frac{3J(J-1)}{2(2J-1)(2J+1)}, \tag{16}$$

for the Q($\Delta J = 0, L = 2$) transitions:

$$C(J\ 2\ J;00)^2 = \frac{J(J+1)}{(2J-1)(2J+3)}, \tag{17}$$

and for the S($\Delta J = 2, L = 2$) transitions:

$$C(J\ 2\ [J+2];00)^2 = \frac{3(J+1)(J+2)}{2(2J+1)(2J+3)}. \tag{18}$$

The term Y_{Lm} in equation (8) is small compared with X_{Lm} and accounts for the contribution of the anisotropy of the polarizability of the L-pole transitions, and is given by

$$\begin{aligned}Y_{Lm} = P_{J_1}P_{J_2}\Bigg[&\frac{2}{9}C(J_1LJ_1';00)^2C(J_22J_2';00)^2\\ &\times \langle v_1J_1 \mid Q_{L_1} \mid v_1'J_1'\rangle^2\langle v_2J_2 \mid \gamma_2 \mid v_2'J_2'\rangle^2\\ &+ \frac{2}{9}C(J_12J_1';00)^2C(J_2LJ_2';00)^2\\ &\times \langle v_2J_2 \mid Q_{L_2} \mid v_2'J_2'\rangle^2\langle v_1J_1 \mid \gamma_1 \mid v_1'J_1'\rangle^2\\ &- \frac{4}{15}C(J_12J_1';00)^2C(J_22J_2';00)^2\\ &\times \langle v_1J_1 \mid Q_{L_1} \mid v_1'J_1'\rangle\langle v_2J_2 \mid \gamma_2 \mid v_2'J_2'\rangle\\ &\times \langle v_2J_2 \mid Q_{L_2} \mid v_2'J_2'\rangle\langle v_1J_1 \mid \gamma_1 \mid v_1'J_1'\rangle\Bigg].\end{aligned} \tag{19}$$

In equations (8) and (19) subscripts 1 and 2 refer to the two colliding molecules 1 and 2, vJ and $v'J'$ are their initial and final vibrational and rotational quantum numbers, and $\langle|Q|\rangle$, $\langle|\alpha|\rangle$ and $\langle|\gamma|\rangle$ are the matrix elements of the 2^L-pole induction, isotropic polarizability and anisotropic polarizability respectively. These values for D_2 were given by Hunt et al. [40].

5 The Birnbaum-Cohen line-shape function

The dimensionless absorption coefficient $\widetilde{\alpha}(\nu)$ for the quadrupolar transitions at a wave number ν of a band is represented by Birnbaum-Cohen line-shape function [29] as

$$\widetilde{\alpha}(\nu) = \sum_m \widetilde{\alpha}_{qm}^{BC} W_q^{BC}(\Delta\nu), \tag{20}$$

where the detailed balance condition is inherently included in $W_q^{BC}(\Delta\nu)$ which is given by

$$W_q^{BC}(\Delta\nu) = \frac{1}{2\pi^2 c\delta_1} \exp\left(\frac{\delta_1}{\delta_2}\right) \exp\left(\frac{hc\Delta\nu}{2kT}\right) \frac{zK_1(z)}{1+(\Delta\nu/\delta_1)^2}, \tag{21}$$

$\widetilde{\alpha}_m^{BC}$ is the calculated intensity for each transition m using equation (7), with

$$z = \left[1+(\Delta\nu\delta_1)^2\right]^{1/2} \left[\left(\frac{\delta_1}{\delta_2}\right)^2 + \left(\frac{hc\delta_1}{2\pi kT}\right)^2\right]^{1/2}. \tag{22}$$

Here $K_1(z)$ is a modified Bessel function of the second kind of order 1 and δ_1 and δ_2 are the parameters of the line shape. These parameters are connected with the characteristic times in the dipole moment correlation function by $\tau_1 = 1/(2\pi c\delta_1)$ and $\tau_2 = 1/(2\pi c\delta_2)$. This function was found to give an excellent fit of the calculated profile with the observed profile, particularly in the wings.

6 Absorption profiles and their analysis

In the present investigation the CIA spectra of the transitions of $D_2(\Delta v = 2 \longleftarrow 0) + D_2(J' \longleftarrow J'')$ and $D_2(\Delta v = 1 \longleftarrow 0) + D_2(\Delta v = 1 \longleftarrow 0)$ were recorded at 77, 201 and 298 K in the spectral region 5250−7250 cm^{-1}. Figures 1, 2 and 3 show plots of $\ln(I_0(\nu)/I(\nu))$ versus the wavenumber $\nu(cm^{-1})$, for three representative absorption profiles of the first overtone band of D_2–D_2 at 77, 201 and 298 K respectively. The positions of the transitions $O_2(3)$, $O_2(2)$, $Q_2(5)$ to $Q_2(0)$ and $S_2(0)$ to $S_2(4)$ are marked along the wavenumber axis. The main feature of these profiles is the absence of the dip in the Q branch unlike in the fundamental band of pure D_2. Observed absorption peaks of the profiles in these figures are marked with identification numbers. There are four strong broad peaks numbered from 3 to 6, these peaks become narrower with decreasing temperature because the relative translational energy of the colliding pair is smaller at lower temperature and hence the collision duration is relatively large. Also peak number 4 intensity increases rapidly with decreasing temperature, this result also appeared in Gillard's work [26]. It is clear that none of these peaks correspond to any of the calculated single transition wave number. These peaks can be interpreted as a summation of two profiles, namely, a transition of the type $X_2(J) + X_0(J)$ and the type $X_1(J) + X_1(J)$ transition, where X is $O(\Delta J = -2)$, $Q(\Delta J = 0)$ or $S(\Delta J = 2)$ transition, the subscript 0, 1 and 2 means pure rotation or orientation transition $\Delta v = 0$, fundamental transition $\Delta v = 1$ and first overtone transition $\Delta v = 2$, respectively, and J is the lowest rotational

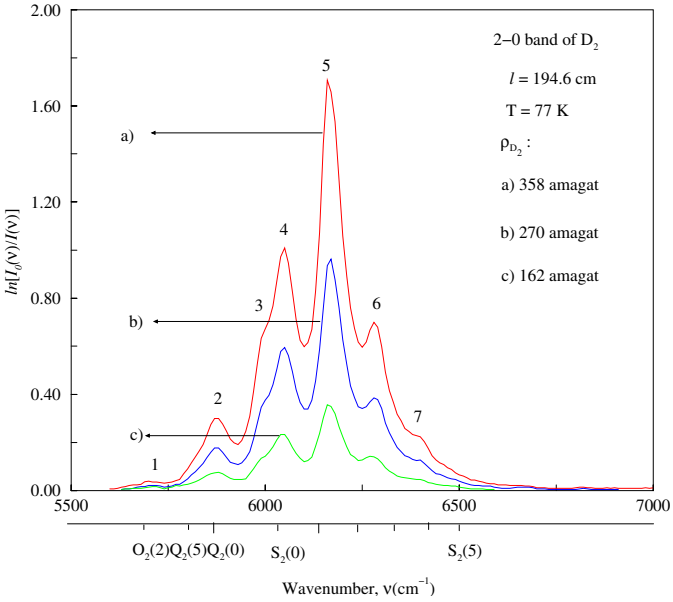

Fig. 1. Three typical enhancement absorption profiles of the first overtone band of pure D_2 at 77 K [26].

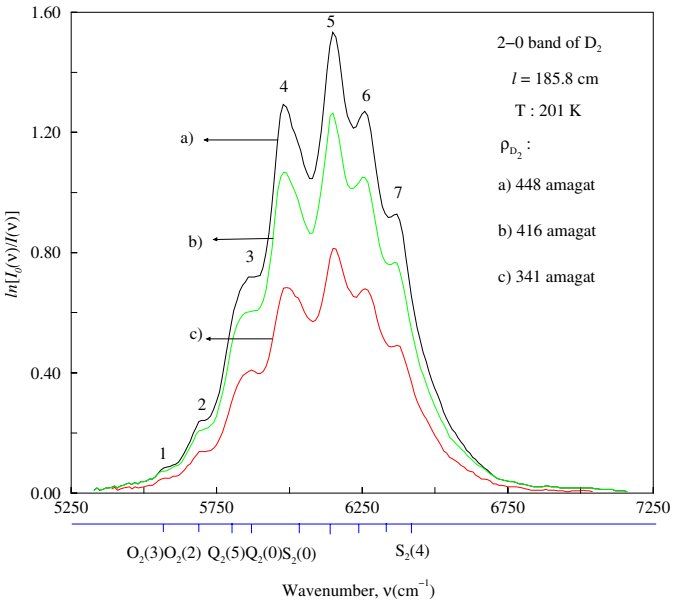

Fig. 2. Three typical enhancement absorption profiles of the first overtone band of pure D_2 at 201 K.

Table 2. Absorption coefficients of the first overtone band of pure D_2 and pure H_2 [41] at different temperatures.

Gas	Temperature (K)	α_1 ($cm^{-2}\,amagat^{-2}$) $\times10^{-5}$	$\widetilde{\alpha}_1$ ($cm^6\,s^{-1}$) $\times10^{-37}$	$\widetilde{\alpha}_1$ [a] ($cm^6\,s^{-1}$) $\times10^{-37}$	$\widetilde{\alpha}_1$ [b] ($cm^6\,s^{-1}$) $\times10^{-37}$	α_2 ($cm^{-2}\,amagat^{-3}$) $\times10^{-9}$	$\widetilde{\alpha}_2$ ($cm^9\,s^{-1}$) $\times10^{-60}$
D_2	77	1.50 ± 0.05 [c]	1.02 ± 0.03	1.04	1.17	0.73 ± 0.20	0.18 ± 0.09
D_2	201	1.88 ± 0.05	1.28 ± 0.03	1.27	1.24	3.6 ± 1.4	0.91 ± 0.04
D_2	298	1.93 ± 0.03	1.31 ± 0.02	1.18	1.30	9 ± 1	2.2 ± 0.1
D_2	298	2.10 ± 0.07 [d]	1.43 [d]				
H_2	77	4.31 ± 0.09 [e]	2.1 [e]	–	–	–0.03 ± 0.3 [e]	–
H_2	80	3.5 [f]		–	–	–	–
H_2	201	4.99 ± 0.08 [e]	2.44 [e]	–		1.9 ± .3 [e]	–
H_2	295	5.8 ± 0.1 [e f]	2.86 [e]	–	–	1.2 ± 0.3 [a]	–
H_2	300	6.2 [f]	–	–	–	–	–

[a]Experimental results from reference [26], the third value at 295 K. [b]Theoretical calculations from reference [26]. [c]The errors quoted are standard deviations. [d]From reference [23]. [e]From reference [41]. [f]From reference [7].

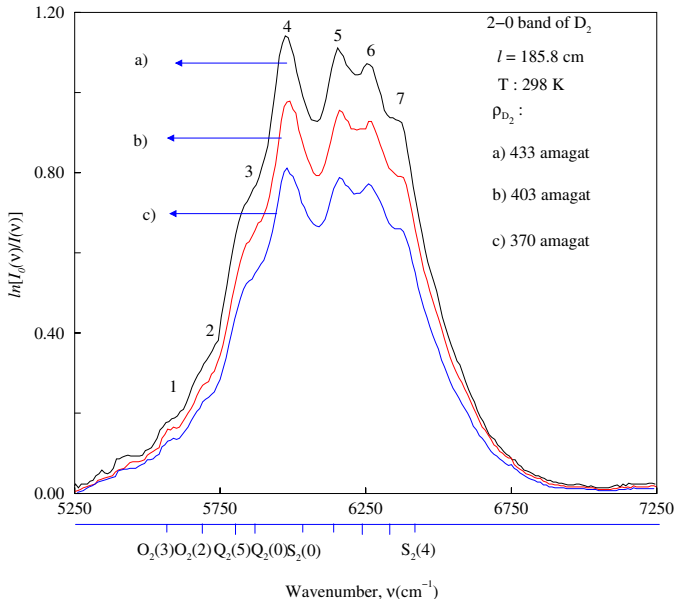

Fig. 3. Three typical enhancement absorption profiles of the first overtone band of pure D_2 at 298 K.

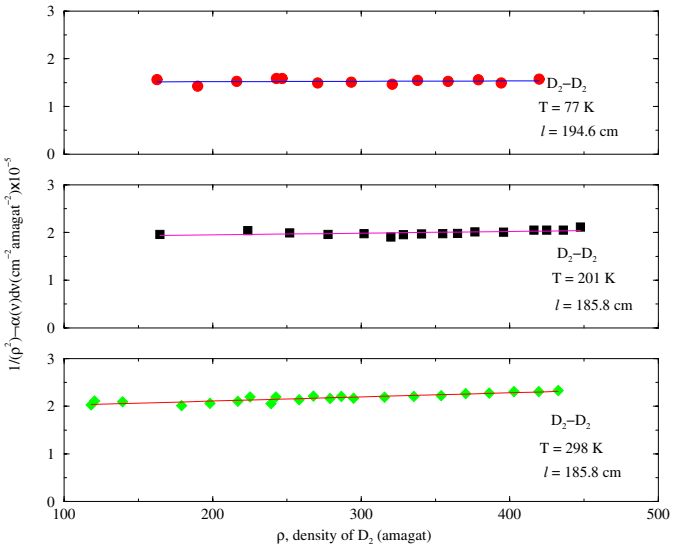

Fig. 4. Plots of $(1/\rho^2)\int \alpha_{en}(\nu)d\nu$ against ρ for the first overtone band of D_2 at 77, 201 and 298 K.

level. All such combinations are listed in Table 1. For example peak four in Figure 1 is formed of the following transitions: $Q_1(J)+Q_1(J)$, $S_1(J)+O_1(J)$, $Q_2(J)+Q_0(J)$, $Q_2(J)+S_0(0)$ and $S_2(0)+Q_0(J)$. While peak five is formed of the following transitions: $S_1(0)+Q_1(J)$, $Q_2(J)+S_0(1)$ $S_2(1)+Q_0(J)$. Watanabe [10] used similar method to analyze the first overtone band of H_2. He mentioned that each of the colliding molecules simultaneously undergoes a vibrational or vibrational-orientational transition of identical energy.

Figure 4 shows three plots of $(1/\rho^2)\int \alpha(\nu)d\nu$ versus ρ at 77, 201 and 298 K, which were used to calculate the absorption coefficients. The plots give straight lines, with the intercept representing the binary absorption coefficient α_1 and the slope representing the ternary coefficient α_2. These coefficients α_1 and α_2 were determined and listed in Table 2. These values were smaller than the values determined for H_2 at the same temperatures. This is because many factors one of them is the rotational constants of hydrogen larger than the rotational constants of deuterium, (see the same table). It can be seen that the ternary absorption coefficients are four orders of magnitude smaller than the binary absorption coefficients, so their contribution to the absorption band is very small at the densities studied here. This result is also clear in the H_2 case. The possible transitions in the region of study 5250 to 7250 cm^{-1} with considerable intensity ($v' = 2 \leftarrow v = 0$) and ($v' = 1 \leftarrow v = 0$) are listed in Table 2. The corresponding transition intensities calculated using equation (7) were used in equation (20) to calculate the total theoretical profile. Examples of the comparison between the experimental and

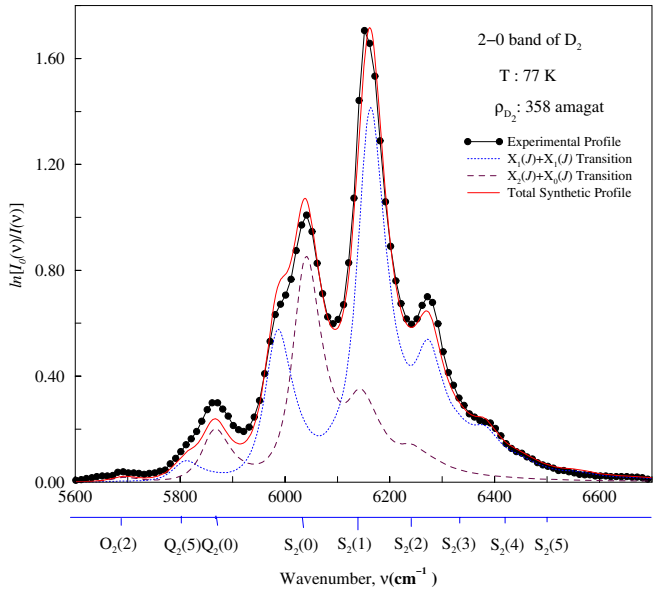

Fig. 5. Analysis of an enhancement absorption profile of the first overtone band of D_2 at 77 K. The open circle symbol is the experimental profile [26], the dashed curve represents the computed double-transition quadrupolar components $D_2(v' = 2, J' \leftarrow v = 0, J) + D_2(v' = 0, J' \leftarrow v = 0, J)$, the dot curve represents the computed individual double-transition quadrupolar components $D_2(v' = 1, J' \leftarrow v = 0, J) + D_2(v' = 1, J' \leftarrow v = 0, J)$ and the solid line curve is the summation of these i.e. the total synthetic profile. See the text for further details.

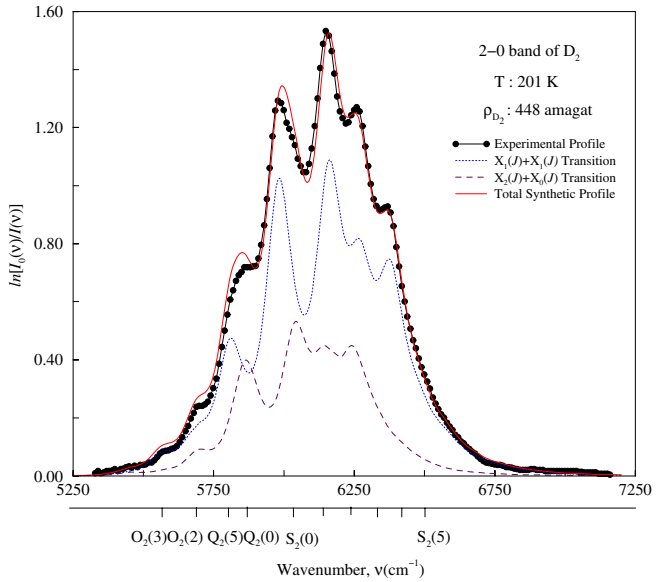

Fig. 6. Analysis of an enhancement absorption profile of the first overtone band of D_2 at 201 K. The circle symbol is the experimental profile, the dashed curve represents the computed double-transition quadrupolar components $D_2(v' = 2, J' \leftarrow v = 0, J) + D_2(v' = 0, J' \leftarrow v = 0, J)$, the dot curve represents the computed individual double-transition quadrupolar components $D_2(v' = 1, J' \leftarrow v = 0, J) + D_2(v' = 1, J' \leftarrow v = 0, J)$ and the solid line curve is the summation of these i.e. the total synthetic profile.

the theoretical profiles at 77, 201 and 298 K are shown in Figures 5, 6 and 7, respectively. It can be seen that the theoretical profile agrees very well with the experimental profile, and the area agreement is better than 97% in the three cases. Figure 5 shows the experimental profile of 358 amagat at 77 K which is represented by the circle symbol [26]. The dashed curve represents the computed double-transition quadrupolar components $D_2(v' = 2, J' \leftarrow v = 0, J) + D_2(v' = 0, J' \leftarrow v = 0, J)$, the dot curve represents the computed individual double-transition quadrupolar components $D_2(v' = 1, J' \leftarrow v = 0, J) + D_2(v' = 1, J' \leftarrow v = 0, J)$ and the solid line curve is the summation of these i.e. the total synthetic profile. The average values of the parameters δ_1, δ_2, τ_1 and τ_2 of the line shape function for the best fits for profiles were determined and are given in Table 3. This table shows that the percentage of the contribution of the vibration–vibration transition $(v' = 1 \leftarrow v = 0) + (v' = 1 \leftarrow v = 0)$ of the two colliding molecules increases as the temperature increases, while the percentage of the contribution of the vibration–rotation and vibration–orientation $(v' = 2 \leftarrow v = 0) + (v' = 0 \leftarrow v = 0)$ decreases as the temperature increases. The percentage of the contribution of $X_1(J) + X_1(J)$ to $X_2(J) + X_0(J)$ is 65 to 35 69 to 31% and 72 to 28% at 77, 201 and 298 K, respectively. Also Figure 8 shows that δ_1 the halfwidth parameter is proportional linearly with the root square of the temperature.

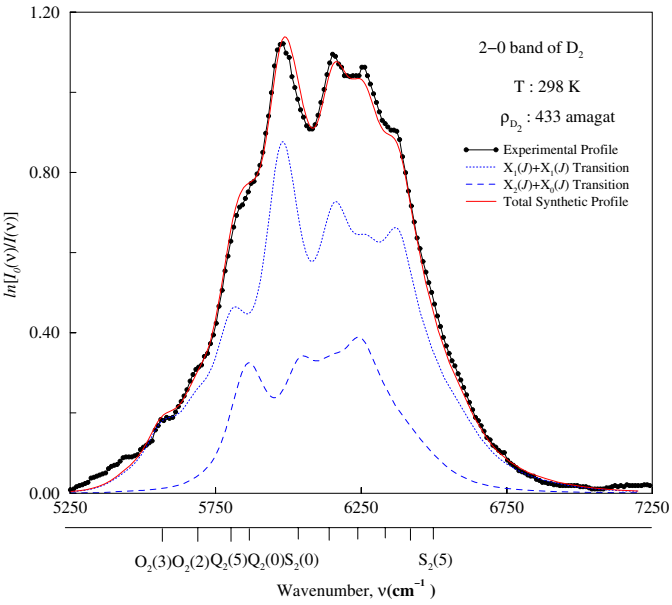

Fig. 7. Analysis of an enhancement absorption profile of the first overtone band of D_2 at 298 K. The circle symbol is the experimental profile, the dashed curve represents the computed double-transition quadrupolar components $D_2(v' = 2, J' \leftarrow v = 0, J) + D_2(v' = 0, J' \leftarrow v = 0, J)$, the dot curve represents the computed individual double-transition quadrupolar components $D_2(v' = 1, J' \leftarrow v = 0, J) + D_2(v' = 1, J' \leftarrow v = 0, J)$ and the solid line curve is the summation of these i.e. the total synthetic profile.

Table 3. Birnbaum-Cohen line-shape parameters for the first overtone band of pure D_2 at different temperatures.

Temperature	Transition	Percentage	Number of profiles	δ_1 (cm^{-1})	δ_2 (cm^{-1})	τ_1 [a] (10^{-14} s)	τ_2 [a] (10^{-14} s)
77 K	$X_1 + X_1$ [b]	65	13	33.6 ± 0.8 [d]	88 ± 5	15.8 ± 0.4	6.0 ± 0.3
	$X_2 + X_0$	35	13				
	theory/exp. [c]	97	13				
201 K	$X_1 + X_1$	69	16	61 ± 1	150 ± 7	8.7 ± 0.1	3.5 ± 0.2
	$X_2 + X_0$	31	16				
	theory/exp. [c]	98	16				
298 K	$X_1 + X_1$	72	22	83 ± 2	170 ± 10	6.4 ± 0.2	3.1 ± 0.2
	$X_2 + X_0$	28	22				
	theory/exp. [c]	99	22				

[a] $\tau_i = 1/(2\pi c\delta_i)$. [b] X could be O, Q or S transition. [c] The theoretical to experimental ratio of the fitted area. [d] The errors listed are standard deviations.

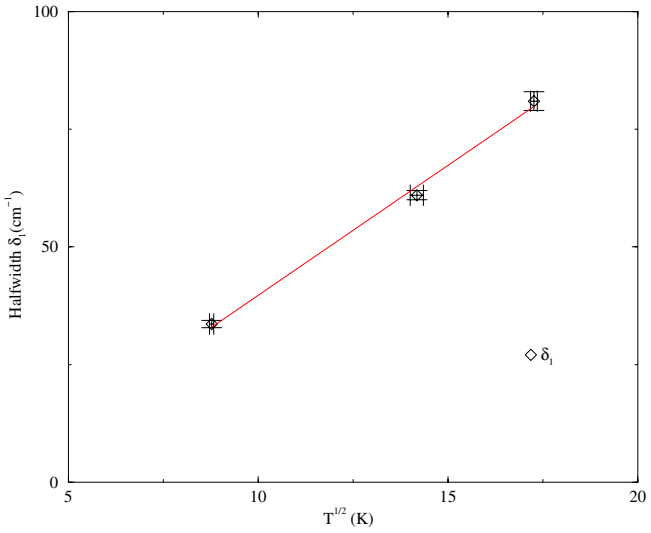

Fig. 8. A plot of the halfwidth parameter δ_1 (cm^{-1}) versus $\sqrt{T}$ ($\sqrt{K}$). The error bars represent the maximum experimental deviations.

7 Conclusions

The observed spectra confirm that the isotropic overlap induction mechanism is absent in the first overtone band of pure D_2 unlike in the CIA spectra of the fundamental band of D_2. They are formed of 267 quadrupolar transitions of the type $X_2(J) + X_0(J)$ and the type $X_1(J) + X_1(J)$, respectively, where X represents $O(\Delta J = J' - J'' = -2)$, $Q(\Delta J = 0)$ or $S(\Delta J = 2)$ transitions, at room temperature. The synthetic profiles agree well with the experimental profiles within 97%. The line shape fitting parameters δ_1, δ_2, τ_1 and τ_2 were determined. The absorption coefficients were determined and the effect of the ternary is found to be small compared with the binary.

This work was supported in part by a grant (A-2440) awarded to S.P. Reddy from Natural Sciences and Engineering Research Council of Canada.

References

1. H.L. Welsh, MTP Intern. Rev. Sci. Phys. Chem. **3**, 33 (1972)
2. L.M. Trafton, *Molecular Complexes in Earths, Planetary, cometary, and interstellar atmospheres* (World Scientific, Singapore, 1998), Chap. 6, pp. 177–193
3. A.R.W. McKellar, H.L. Welsh, Proc. Roy. Soc. Lond. A **322**, 421 (1971)
4. A. Borysow, U.G. Jorgensen, C. Zheng, Astron. Astrophys. **324**, 185 (1997)
5. A. Borysow, J. Borysow, Y. Fu, Icarus **145**, 601 (2000)
6. A. Borysow, Astron. Astrophys. **390**, 779 (2002)
7. H.L. Welsh, M.F. Crawford, J.C.F. MacDonald, D.A. Chisholm, Phys. Rev. **83**, 1264 (1951)
8. W.F. Hare, H.L. Welsh, Can. J. Phys. **36**, 88 (1958)
9. A. Watanabe, J.L. Hunt, H.L. Welsh, Can. J. Phys. **49**, 860 (1971)
10. A. Watanabe, Can. J. Phys. **49**, 1320 (1971)
11. P.M. Silvaggio, D. Goorvitch, R.W. Boese, J. Quant. Spect. Rad. Transfer **26**, 103 (1981)
12. A.R.W. McKellar, Can. J. Phys. **66**, 155 (1988)
13. W. Meyer, A. Borysow, L. Frommhold, Phys. Rev. A **47**, 4065 (1993)
14. S.P. Reddy, F. Xiang, G. Varghese, Phys. Rev. Lett. **74**, 367 (1995)
15. A.R.W. McKellar, M.J. Clouter, Can. J. Phys. **72**, 51 (1994)
16. M. Gustafsson, L. Frommhold, D. Bailly, J. Bouanich, C. Brodbeck, J. Chem. Phys. **119**, 12264 (2003)
17. A.R.W. McKellar, J. Chem. Phys. **105**, 2628 (1996)
18. A.R.W. McKellar, J. Chem. Phys. **122**, 174313 (2005)
19. A.R.W. McKellar, J. Chem. Phys. **122**, 84320 (2005)
20. S.P. Reddy, C.W. Cho, Can. J. Phys. **43**, 2331 (1965)
21. A. Watanabe, H.L. Welsh, Can. J. Phys. **43**, 818 (1965)
22. S.T. Pai, S.P. Reddy, C.W. Cho, Can. J. Phys. **44**, 2893 (1966)
23. S.P. Reddy, C.Z. Kuo, J. Mol. Spectr. **37**, 327 (1971)
24. W.E. Russell, S.P. Reddy, C.W. Cho, J. Mol. Spectr. **52**, 72 (1974)

25. R.J. Penney, R.D.G. Prasad, S.P. Reddy, Chem. Phys. **77**, 131 (1982)
26. P.G. Gillard, Memorial University of Newfoundland (1983)
27. M. Abu-Kharma, G. Varghese, S.P. Reddy, J. Mol. Spect. **232**, 369 (2005)
28. M. Abu-Kharma, S.P. Reddy, J. Mol. Spect. **233**, 133 (2005)
29. G. Birnbaum, E.R. Cohen, Can. J. Phys. **54**, 593 (1976)
30. K.P. Huber, G. Herzberg, *Constants of Diatomic Molecules* (Van Nostrand Reinhold Comp., 1979), Vol. 4, p. 240
31. A. Michels, W.D. Graaff, T. Wassenaar, J.M. Levelt, P. Louwerse, Physica **25**, 25 (1959)
32. J. van Kranendonk, Physica **24**, 347 (1958)
33. J. van Kranendonk, Physica **25**, 337 (1959)
34. J. van Kranendonk, Can. J. Phys. **46**, 1173 (1968)
35. J. van Kranendonk, Physica **73**, 156 (1974)
36. G. Karl, J.D. Poll, L. Wolniewicz, Can. J. Phys. **53**, 1781 (1975)
37. J.D. Poll, J.L. Hunt, Can. J. Phys. **54**, 461 (1976)
38. J.C. Lewis, in *Phenomena Induced by Intermolecular Interactions*, edited by G. Birnbaum (Plenum, New York, 1985), pp. 215–257
39. S.P. Reddy, in *Phenomena Induced by Intermolecular Interactions*, edited by G. Birnbaum (Plenum, New York, 1985), pp. 129–167
40. J.L. Hunt, J.D. Poll, L. Wolniewicz, Can. J. Phys. **62**, 1719 (1984)
41. E. van Nostrand, Memorial University of Newfoundland (1983)